Journal of Structural Geology 30 (2008) 818–826

Contents lists available at ScienceDirect

Journal of Structural Geology

journal homepage: www.elsevier.com/locate/jsg

Transpressional deformations within the Sanandaj–Sirjan metamorphic belt (Zagros Mountains, Iran)

Khalil Sarkarinejad [a], Ali Faghih [a,b,*], Bernhard Grasemann [b]

[a] Department of Earth Sciences, College of Sciences, Shiraz University, Shiraz, Iran
[b] Department of Geodynamics and Sedimentology, University of Vienna, Vienna, Austria

ARTICLE INFO

Article history:
Received 28 August 2007
Received in revised form 25 February 2008
Accepted 9 March 2008
Available online 20 March 2008

Keywords:
Transpression
Quantitative kinematic analysis
Sanandaj–Sirjan metamorphic belt
Zagros
Iran

ABSTRACT

Polyphase deformation structures of the Sanandaj–Sirjan metamorphic belt in the Neyriz area (Zagros Mountains, Iran) are consistent with dextral transpressional deformation, which is related to the oblique collision between the African–Arabian continent and the Iranian microcontinent. The collision started in the Late-Cretaceous and is continuing to the present day. Quantitative kinematic analyses quartz textures suggest localized shear zones deformed with a significant pure shear component. Spatial orientation of lineation and semi-quantitative kinematic indicators indicate shear zone parallel stretching and shear zone perpendicular shortening. The occurrence of a horizontal stretching component parallel to the deformation zone boundary allows a kinematic model of combined transpression and lateral extrusion for this part of the Zagros orogeny.

1. Introduction

Transpressional deformation (Harland, 1971) is the simultaneous occurrence of strike–slip shearing and shear zone normal shortening and has been considered as an important style of the deformation in the regions of oblique convergence (e.g. Sanderson and Marchini, 1984; Teyssier et al., 1995; Dewey et al., 1998; Lin et al., 1998; Jones et al., 2004). Areas of transpression record structures such as mineral lineations, folds, foliations and secondary shear zones with spatial orientations that may vary along strike and dip of the transpression zone (Tikoff and Teyssier, 1994; Fossen and Tikoff, 1998). The simplest types of transpression models involve homogeneous deformation by a combination of simple and pure shear. In such a general shear model (Fig. 1a) the direction of the vorticity vector is a direction of no incremental strain with shortening perpendicular to the transpression zone that is volumetrically balanced by stretching parallel to the laterally unconfined shearing direction (Ramberg, 1975). In contrast to plain strain models, Sanderson and Marchini (1984) investigated in their model a vertical laterally and basally confined shear zone in which the transpression zone is subjected to strike–slip simple shearing, shortening perpendicular to the shear zone and vertical extrusion of the material (Fig. 1b). Fossen and Tikoff (1993) introduced a modification of this model considering a deformation matrix for simultaneous simple-, pure-shearing and volume change, and its application to transpression–transtension tectonics. Robin and Cruden (1994) developed a model with no-slip boundaries between deforming zone and the wall rocks, resulting in a symmetry variation in strain within the transpression zone (Fig. 1c). Avé Lallemant and Guth (1990) and Jones et al. (1997) introduced an additional component of extension in the horizontal direction that allows for unconfined extrusion of the deformation zone (Fig. 1d). This component enhances the stability of vertical foliation–horizontal lineation in transpression zone (Teyssier and Tikoff, 1999). Jones and Holdsworth (1998), Lin et al. (1998) and Jiang et al. (2001) included vertical displacement of one wall rock relative to the other, resulting in oblique simple shear strain of triclinic symmetry in contrast to previous homogeneous monoclinic flow models (Fig. 1e). Czeck and Hudleston (2003, 2004) proposed a conceptual model of a vertical transpression zone with local non-vertical extrusion and tested this model with analogue experiments. The inclined transpression model of Jones et al. (2004) involves simultaneous pure shearing and strike–slip and dip–slip shearing resulting in triclinic flow (Fig. 1f). Several kinematic studies from transpression zones have been attracted by triclinic flow models mainly because they provide a satisfactory explanation of the observed spatial variations in the foliation, lineation and fold hinge data (e.g. Díaz Azpiroz and Fernández, 2005).

To add more data from natural rocks to the large volume of theoretical work, we focus on the Neyriz area (Iran), where the

* Corresponding author. Department of Earth Sciences, College of Sciences, Shiraz University, Golestan Street, Adabiat Junction, Shiraz 71454, Iran. Tel./fax: +98 711 228 4572.
E-mail address: afaghih@shirazu.ac.ir (A. Faghih).

0191-8141/$ – see front matter © 2008 Elsevier Ltd. All rights reserved.
doi:10.1016/j.jsg.2008.03.003

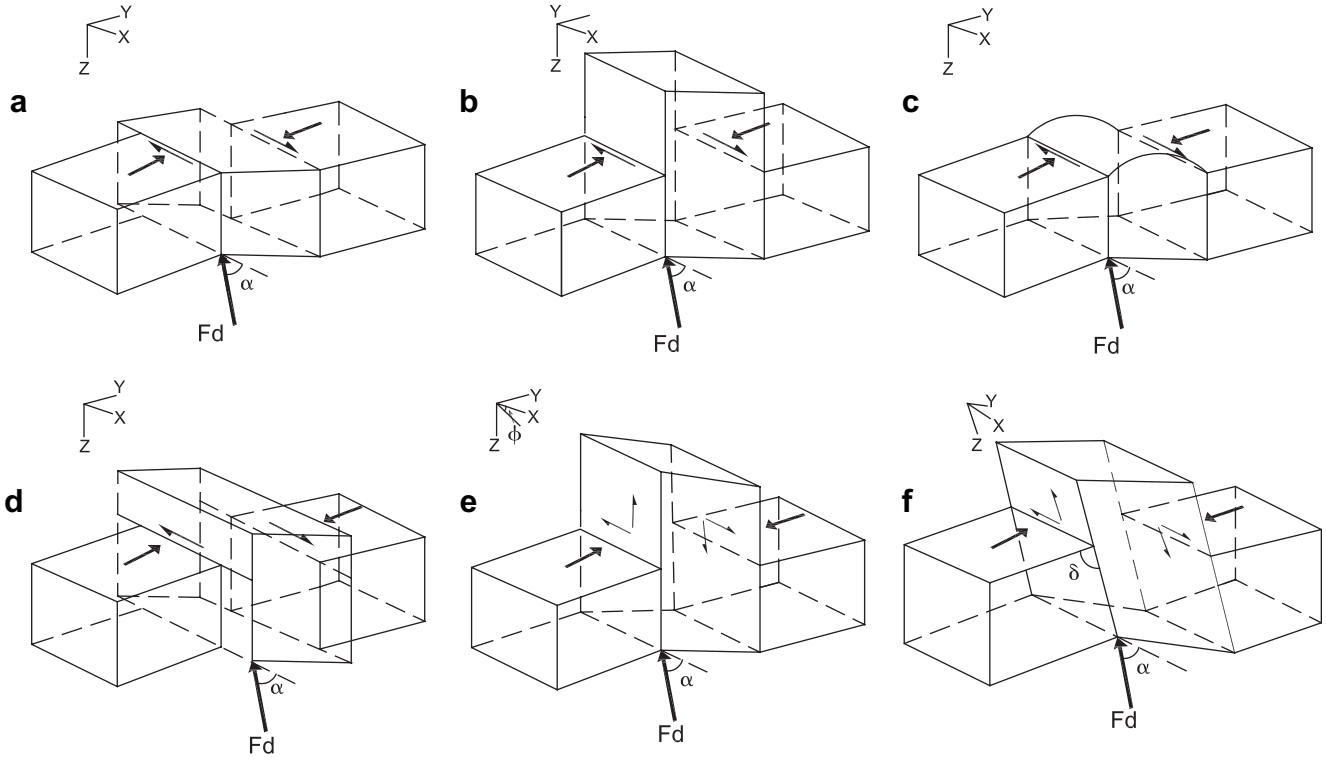

Fig. 1. Different types of transpression models shown in *X*, *Y* and *Z* coordinate system with reference to the transpression zone boundary. The full arrows represent the shortening perpendicular to the transpression zone, associated with the pure shear component. The half arrows mark the shear component. Fd is the convergence vector with angle α to the transpression zone boundary. φ is the angle between the strike of the transpression zone boundary and the orientation of the shear component of strain. δ is the dip of transpression zone boundary. (a) Plane strain general shear. (b) Model of Sanderson and Marchini (1984). (c) Model of Robin and Cruden (1994). (d) Model of Jones et al. (1997). (e) Model of Lin et al. (1998). (f) Model of Jones et al. (2004).

Zagros Suture Zone separates the northeastern end of the African–Arabian continent to the south and the Iranian microcontinent to the north. Based on fieldwork, a detailed quantitative structural analysis for the Sanandaj–Sirjan metamorphic belt in the Neyriz area is presented giving evidence for a dextral extrusive transpression zone.

2. Regional geological setting

The Zagros orogen is a linear collisional orogen and part of the Alpine–Himalayan orogenic belt (e.g. Stöcklin, 1968; Ricou, 1971; Dewey et al., 1973; Berberian and King, 1981; Koop and Stoneley, 1982; Ziegler and Stampfli, 2001; Blanc et al., 2003; McClay et al., 2004). Regional deformation arising from the Late-Cretaceous to Tertiary collision between the African–Arabian continent and the Iranian microcontinent accounts for the lineation, foliation, isoclinal folding, thrusting and large-scale strike–slip faulting associated with crustal shortening in the Zagros orogeny (Alavi, 1994; Sepehr and Cosgrove, 2005; Sarkarinejad and Azizi, 2008). Post-collisional crustal shortening is active to the present day (Jackson and McKenzie, 1984; Talebian and Jackson, 2002; Allen et al., 2004; Regard et al., 2004; Tatar et al., 2004) with a N–S-oriented convergence rate of approximately 20 ± 2 mm yr^{-1} (Vernant et al., 2004; Molinaro et al., 2005).

The study area is located in the Neyriz area, 250 km east from Shiraz in southwestern Iran (Fig. 2). Metamorphosed and deformed rocks of this area are part of the high-pressure/low-temperature Sanandaj–Sirjan metamorphic belt (Alavi, 1994; Sarkarinejad, 1999). The Sanandaj–Sirjan metamorphic belt is a zone of thrust faults that have transported numerous slices of variously metamorphosed Phanerozoic stratigraphic units. Stratigraphic evidence and synorogenic conglomerates indicate that thrusting initiated in the Late-Cretaceous. Shear sense indicators in various parts of the zone reveal top-to-the-SW directed movement (Alavi, 1994, 2004; McQuarrie, 2004). The rocks in the study area consist of mainly mafic and ultramafic rocks of various metamorphic grades such as greenschists, amphibolites, blueschists and eclogites. From northwest (Sanandaj) to southeast (Sirjan), this NW–SE trending Sanandaj–Sirjan belt is about 150–200 km wide, more than 1500 km long and parallels the main regional structures of the Zagros orogen.

3. Deformation history

The Sanandaj–Sirjan metamorphic belt experienced a polyphase deformation history, which is related to collision tectonics. Our structural and microstructural studies focus on the characteristics and spatial orientations of folds, foliations and lineations in order to understand the overprint relationships between these structural elements. Three main deformation phases are distinguished, of which is interpreted to represent kinematically distinct events in the progressively evolving collision zone.

3.1. D1 structures

This first preserved deformation phase, which affected the entire Sanandaj–Sirjan metamorphic belt created a penetrative foliation (S1), mesoscopic isoclinal folds (F1), and penetrative stretching lineation (L1) that is defined by the long axes of top-to-the-SW sheared quartz, feldspar and hornblende. The S1 foliation and metamorphic layering form a continuous moderately NNE-dipping foliation (mean: N75°W, 42°NE) which can be observed throughout the metamorphic rocks of the study area. The mean of the L1 stretching lineation dips with 33° towards N52°E (Fig. 3a).

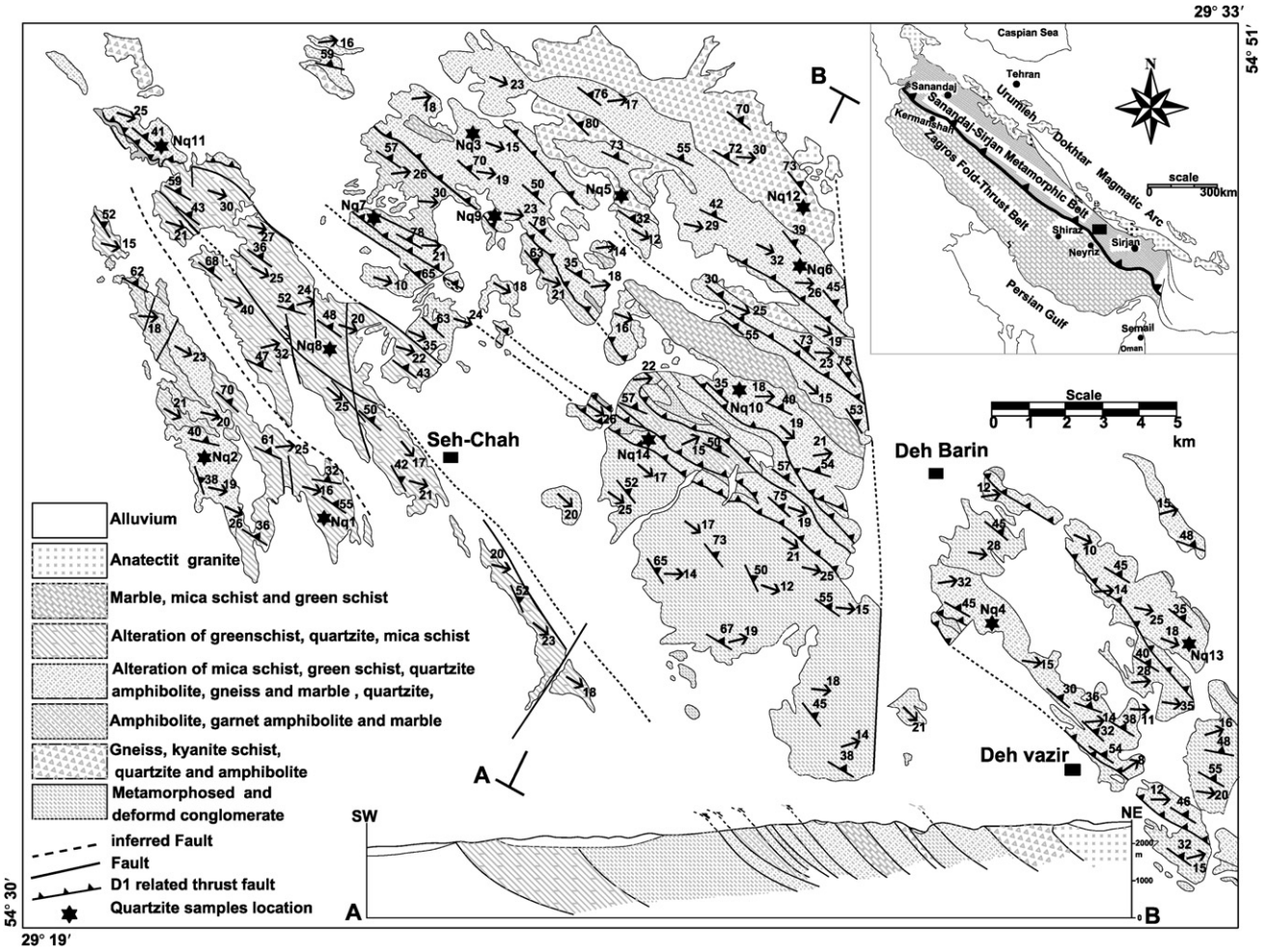

Fig. 2. Geological map of the Neyriz area and a NE–SW oriented cross section, perpendicular to the strike of the main structures. The inset shows a tectonic map of Iran with the Sanandaj–Sirjan metamorphic belt and the location of study area.

Within the S1 mylonitic foliation, isoclinal folds with fold axes F1, roughly parallel to the stretching lineation L1, are preserved (compare Fig. 3a and b). The axial planes of these folds are identical to the mylonitic foliation S1. These partly intrafolial folds suggest a strong shortening component normal to the foliation and are typical for high-strain shear zones (Passchier and Trouw, 2005 and references cited therein).

3.2. D2 structures

The main structures associated with the D2 deformation phase are F2 folds, which fold the S1 mylonitic foliation and therefore refold F1 folds resulting in Type-2 and Type-3 interference patterns (Figs. 3b and 4b). The mean orientation of F2 folds axial planes is 45°, S54°E and partly develops a penetrative S2 foliation or an asymmetrical crenulation cleavage (Fig. 4a) which strikes roughly N50°W and dips moderately to steeply to the NE. F2 fold axes dip moderately towards ESE and are parallel to a crenulation lineation L2 dipping with 25° towards S76°E (Fig. 3c).

Oblique to the D1 foliation, many boudin structures record monoclinic and orthorhombic symmetry (Grasemann and Stüwe, 2001; Goscombe and Passchier, 2003) and are related to the D2 deformation. Different boudin block geometries including domino-, drawn-, shear band- and torn boudins have been preserved (Goscombe et al., 2004). Most of the boudins are arranged in foliation-oblique trains recording monoclinic symmetry (Fig. 5). Boudins, where the inner-boudin zone is oriented perpendicular to the L2 stretching lineation record dextral shear. The amount of stretching and rotation of the boudin trains suggest a stretching component parallel to the shear zone and shortening perpendicular to the shear zone (Müller et al., 2006).

Ductile semi-quantitative D2 kinematic indicators are well developed in the metamorphic rocks of the Sanandaj–Sirjan metamorphic belt. The sense of shear was determined in the field perpendicular to the L2 NW–SE striking lineation and on oriented hand samples and in thin sections. All microscopic and mesoscopic shear sense indicators with monoclinic structures as well as clear stair-stepping geometries or SC/SCʹ fabrics confirm the dextral sense of shear (Fig. 6). Additionally, the dextral D2 shear sense is confirmed by microstructures and microtextures in quartzites. A quantitative kinematic vorticity analysis of D2 quartz textures are discussed below in more detail.

3.3. D3 structures

Whereas D1 and D2 developed under amphibolite and greenschist facies metamorphic conditions, D3 represents an event leading to the development of kink bands, localized shear zones and slickensides along the thrust sheet of the Sanandaj–Sirjan metamorphic belt. Abundant kink bands of several centimetre thickness overprint all other deformation structures (Fig. 4c). The

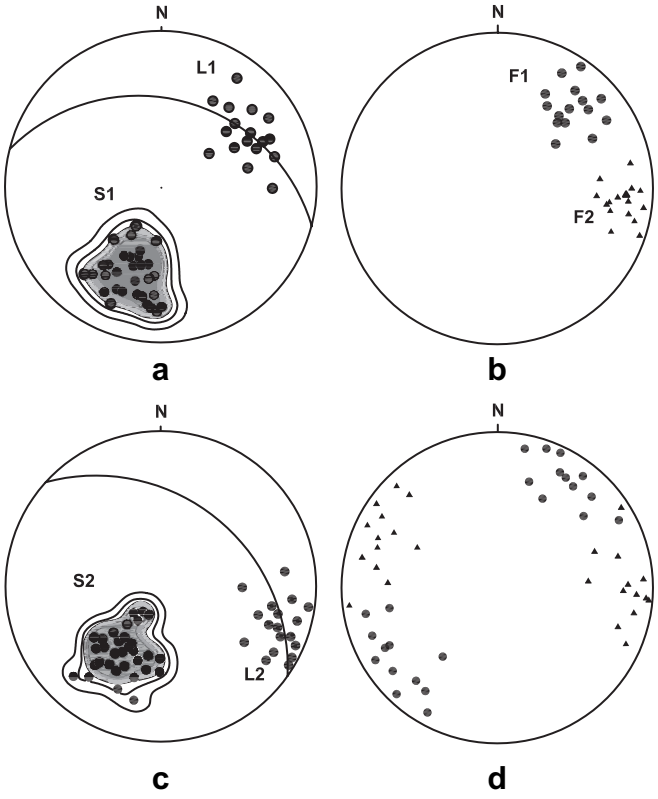

Fig. 3. Lower hemisphere, equal area stereographic projections of D1, D2 and D3 structural elements summarizing the orientation of Lineations (L1 and L2), Foliations (S1 and S2), fold axis (F1 and F2) and kink bands. (a) Poles to S1 foliation which are contoured at 1%, 2%, 4%, 6% and 8% per 1% area and L1 lineation related to D1 deformation event (b) Orientation pattern of F1 and F2 fold axes related to D1 and D2 respectively. (c) Poles to S2 foliation and L2 lineation related to D2 deformation event (d) Poles to D3 related kink bands.

steeply dipping conjugate kink bands strike NW–SE and NNE–SSW respectively (Fig. 3d).

4. D2 quartz textures

Well-developed *c*-axis fabrics in quartz mylonites can be used to characterize the kinematics of the associated flow (Schmid and Casey, 1986). Fourteen samples of quartz mylonites from different structural positions within the Sanandaj–Sirjan metamorphic belt were measured in order to relate the quartz *c*-axis fabrics to the kinematic history. The quartz fabrics were certainly affected by the D1 deformation. However, dynamic recrystallization still took place during the D2 event and therefore the recorded microstructures are considered to reflect mainly D2. D3 did not affect the quartz textures. The location of the samples is given in Fig. 2. Texture analyses of quartz *c*-axes were investigated from using an optical microscope equipped with universal stage. Our *c*-axis measurements are displayed on equal-area, lower hemisphere stereographic projection and contoured using SpheriStat 2.2 for Windows (Fig. 7). In all these projections, the foliation is vertical and stretching lineation within the foliation is NW–SE horizontal. All samples record a well-preserved shape and crystal preferred orientation consistent with a dextral sense of shear. The fabric of the dynamically recrystallized quartz was formed by both subgrain rotation and grain boundary migration (Fig. 8a). From the density distribution, quartz *c*-axis fabrics of the study area can be described as Type-I cross-girdle fabrics with *c*-axis point maxima at high-angle to the foliation trace which are interpreted basal <a> slip system and moderate temperature (i.e. greenschist facies) deformation

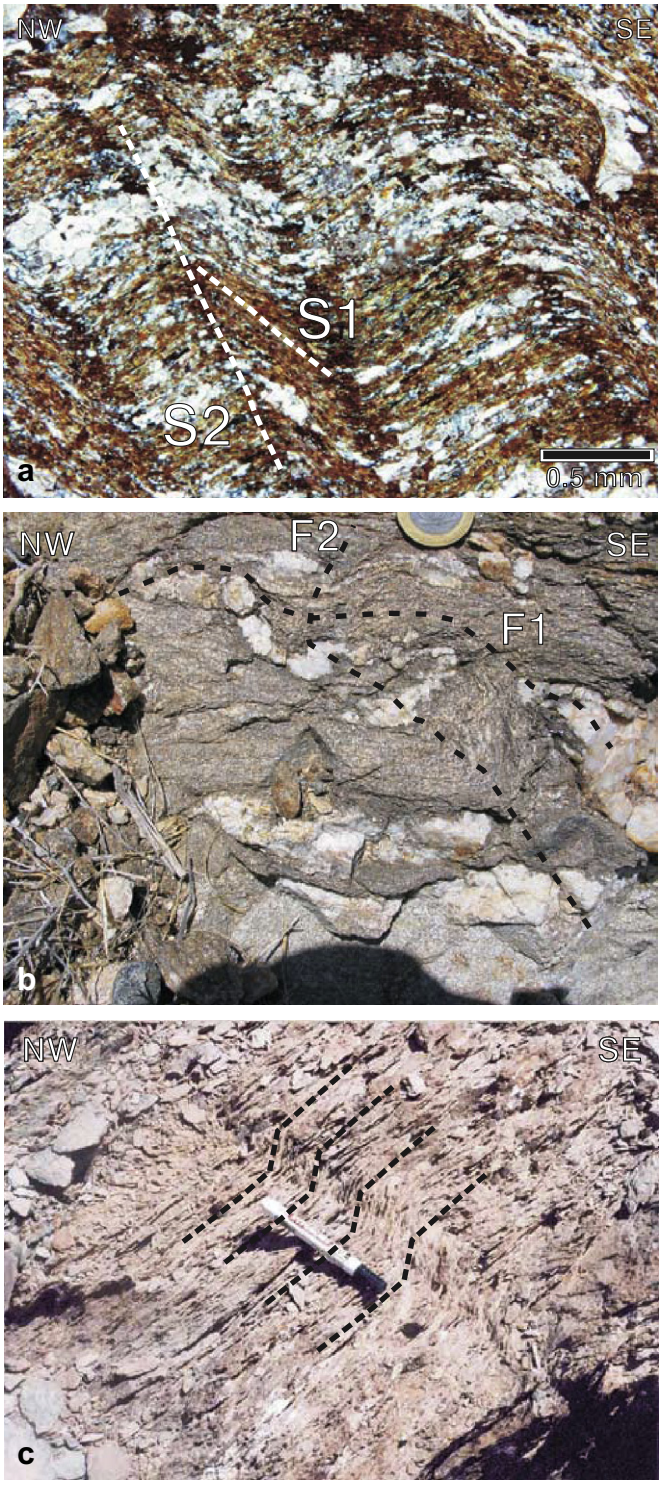

Fig. 4. Mesoscopic and microscopic photograph of D1, D2 and D3 related structures of Sanandaj–Sirjan metamorphic belt in the study area. Micrograph is from thin section cut perpendicular to foliation and parallel to stretching lineation. (a) Optical micrograph of S1 and S2 foliation plane geometry. The S1 foliation is overprinted by the asymmetrical crenulation cleavage (S2) related to D2 deformation event (location: 29°28′05″ N, 54°33′49″ E). (b). Type 2 Interference pattern of D1 related fold (F1) refolded by D2 deformation phase fold (F2). (location: 29°26′12″ N, 54°33′56″ E). (c) Field photo of D3 kink bands displaying late, post-metamorphic deformation (location: 29°22′55″ N, 54°48′03″ E).

conditions. These *c*-axis fabrics show an obliquity of the central girdle segment with respect to the main foliation and lineation, indicating a non-coaxial dextral shear. According to Schmid and Casey (1986) and Law (1990), Type-I cross-girdle of quartz *c*-axis

Fig. 5. Boudin trains formed during D2 deformation indicate dextral shearing and a strong stretching component parallel to the shear zone boundary. Locations: (a) 29°25′08″ N, 54°32′45″ E; (b) 29°20′52″ N, 54°47′35″ E; (c) 29°29′22″ N, 54°37′45″ E; (d) 29°29′37″ N, 54°31′34″ E).

fabrics may be interpreted to indicate plane strain condition during ductile shearing.

5. Kinematic vorticity number (W_k) derived from the D2 quartz textures

Two-dimensional methods of vorticity measurement are valid only for conditions of orthorhombic or monoclinic ductile flow with the vorticity vector parallel to the *Y*-axis of finite strain (Tikoff and Fossen, 1995). The approximately plane-strain conditions we have identified in the study area (as suggested by the Type-I crossed girdle pattern of the quartz *c*-axis, Law, 1990) satisfy the assumptions of the applied method. Therefore we can combine quartz *c*-axis fabrics with R_{xz} (principal normal strain ratio in the *XZ* section) in order to quantitatively estimate W_k values (Wallis, 1995). However, we emphasize that deformation is most likely highly partitioned and incremental and finite strain deformation integrated over the entire transpression zone is certainly non-plane strain or even triclinic.

Several different techniques, mostly using meso- and microscale structures, such as deformed passive markers, rotated porphyroclast, deformed veins and dikes and crystallographic fabrics have been used to measure vorticity (for a review of the methods see Passchier and Trouw, 2005 and references cited therein). In this work, a method based on quartz textures proposed by Wallis (1992, 1995) is used in order to estimate the mean W_k. According to this method, the angle β between the perpendicular to the central girdle of quartz *c*-axis diagram and the foliation is equal to the angle between flow plane and the principal plane of normal strain (Fig. 8b). The angle β is a function of R_{xz} (principal normal strain ratio in the *XZ* section) and W_k, as demonstrated by Wallis (1995):

$$W_k = \sin\left\{\tan^{-1}\left[\frac{\sin(2\beta)}{[(R_{XZ}+1)/(R_{XZ}-1)]-\cos(2\beta)}\right]\right\} \times \frac{(R_{XZ}+1)}{(R_{XZ}-1)} \quad (1)$$

The principal normal strain ratio in the *XZ* section (R_{xz}) was determined using deformed quartz grains. Length to width ratios of quartz grains were determined from measurements, made on *XZ* sections cut parallel to stretching lineation and normal to foliation. R_{xz} was estimated for each sample applying R_f/φ (Ramsay, 1967; Lisle, 1985). The investigated quartz *c*-axes girdles record β angles between 8° and 19° and R_{xz} values between 2.5 and 6, translating into $0.6 < W_k < 0.9$ (mean W_k-value 0.76 ± 0.11, Fig. 8c). We are fully aware that a number of parameters and unknowns affect this calculation (e.g. strain rate, contributions of diffusive mass transfer deformation mechanisms, post-mylonitic recrystallization recovery). Especially for large strains, this angle would be less than 5° for flows with mean vorticity numbers between 0 and 0.9 (Grasemann et al., 1999). However, our results still document a significant component of non-coaxial deformation.

6. Discussion

6.1. Kinematics of deformation events

The leading edge of the northeast-moving African–Arabian continent is marked by the occurrence of the Late-Cretaceous

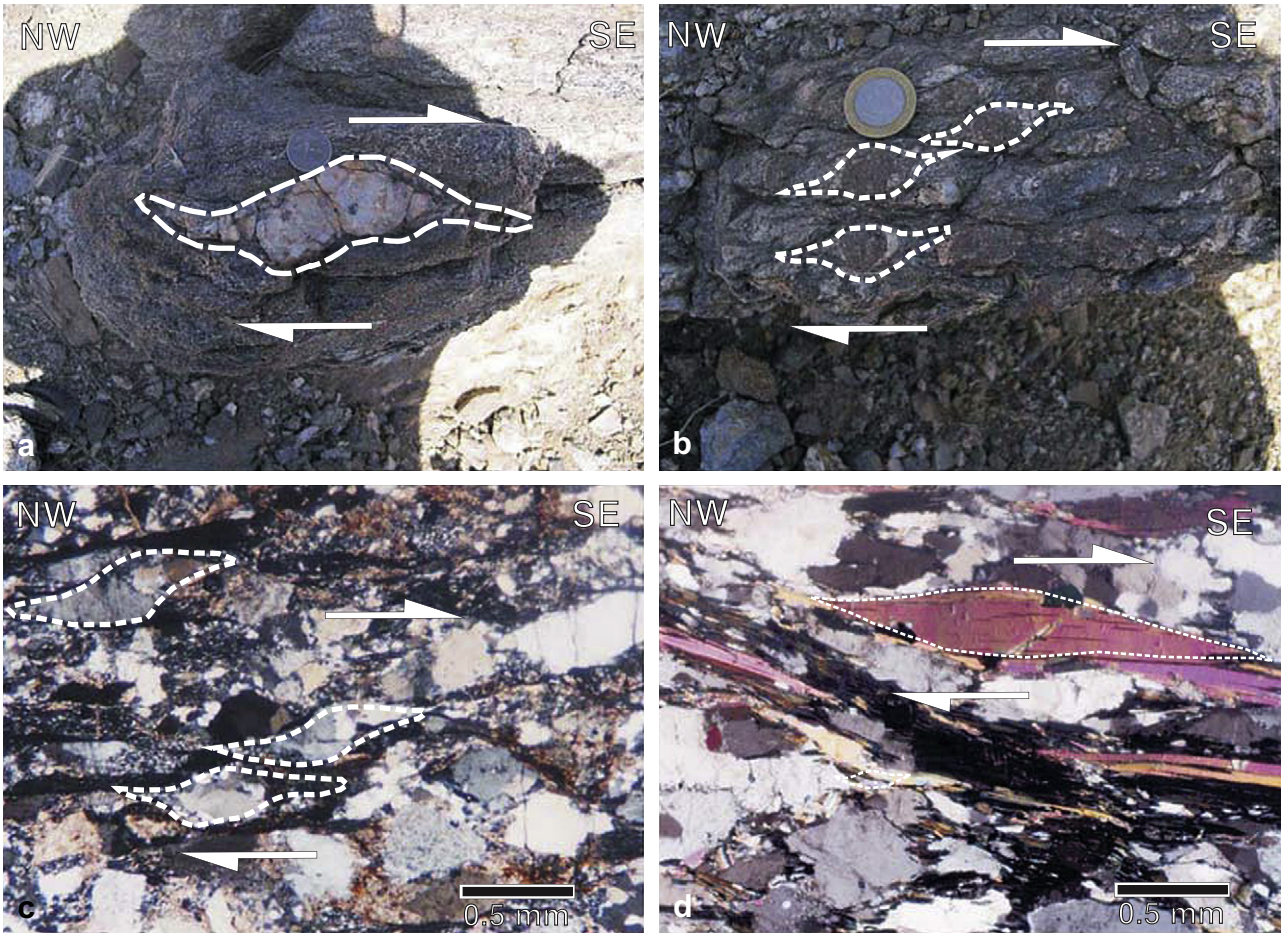

Fig. 6. Microscopic and mesoscopic kinematic indicators of the Sanandaj–Sirjan metamorphic belt in the Neyriz area. All pictures are perpendicular stretching lineation. (a) Field photo of a sigmoidal shaped quartz lense with monoclinic symmetry (location: 29°29′31″ N, 54°36′17″ E). (b) Garnet amphibolite with strain shadows in the extensional quadrants around cm-large garnet grains (location: 29°26′48″ N, 54°32′23″ E). (c) Photomicrograph of quartz grains with monoclinic symmetry in a metamorphosed microconglomerate (location: 29°22′15″ N, 54°48′56″ E). (d) Photomicrograph of mica fish in quartz–feldspar mylonite (location: 29°22′02″ N, 54°36′47″ E). All structures show dextral sense of shear.

ophiolite complex such as Neyriz and Kermanshah in western Iran and Semail ophiolite in Oman along a belt known as the "Croissant ophiolitique" (Ricou, 1971). The Neyriz ophiolite occurs along the NW–SE trending Zagros Thrust System (Stöcklin, 1968; Berberian and King, 1981; Alavi, 1994; Agard et al., 2005; Sarkarinejad and Azizi, 2008) in the Zagros Range between the Sanandaj–Sirjan metamorphic belt to the northeast, and the Zagros Fold- and Thrust-Belt to southwest and represents the Zagros Suture Zone

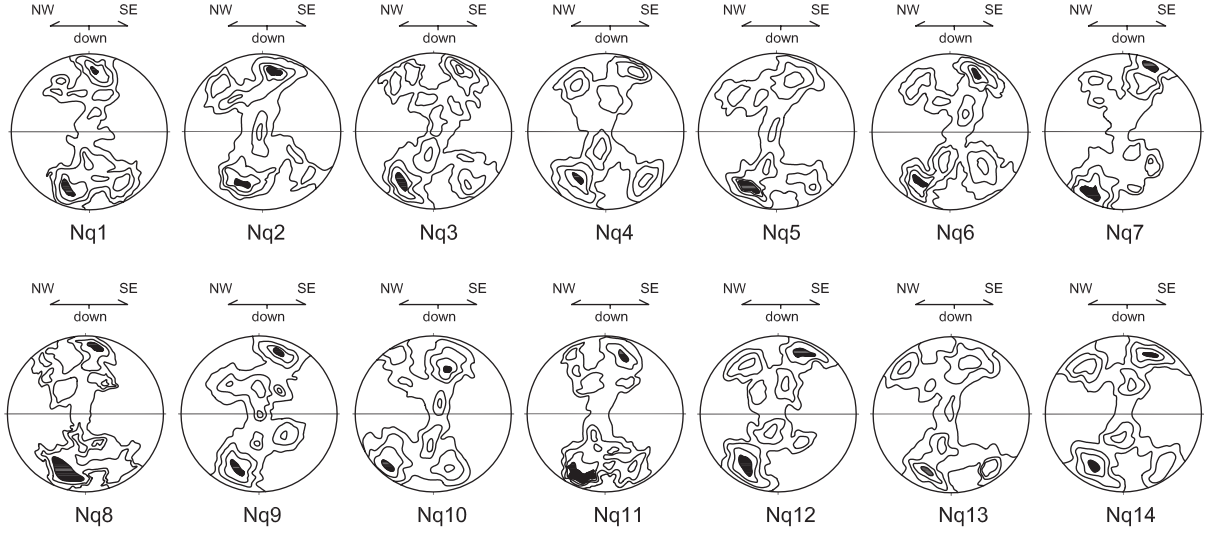

Fig. 7. Lower hemisphere, equal area projection of quartz *c*-axis fabrics. The location of the quartzite samples have displayed in Fig. 2. The texture analyses of quartz *c*-axis were carried out using an optical microscope and an universal stage. In all these projections, the foliation is vertical and stretching lineation within the foliation is horizontal. 250 or more quartz *c*-axis orientation were measured in each sample.

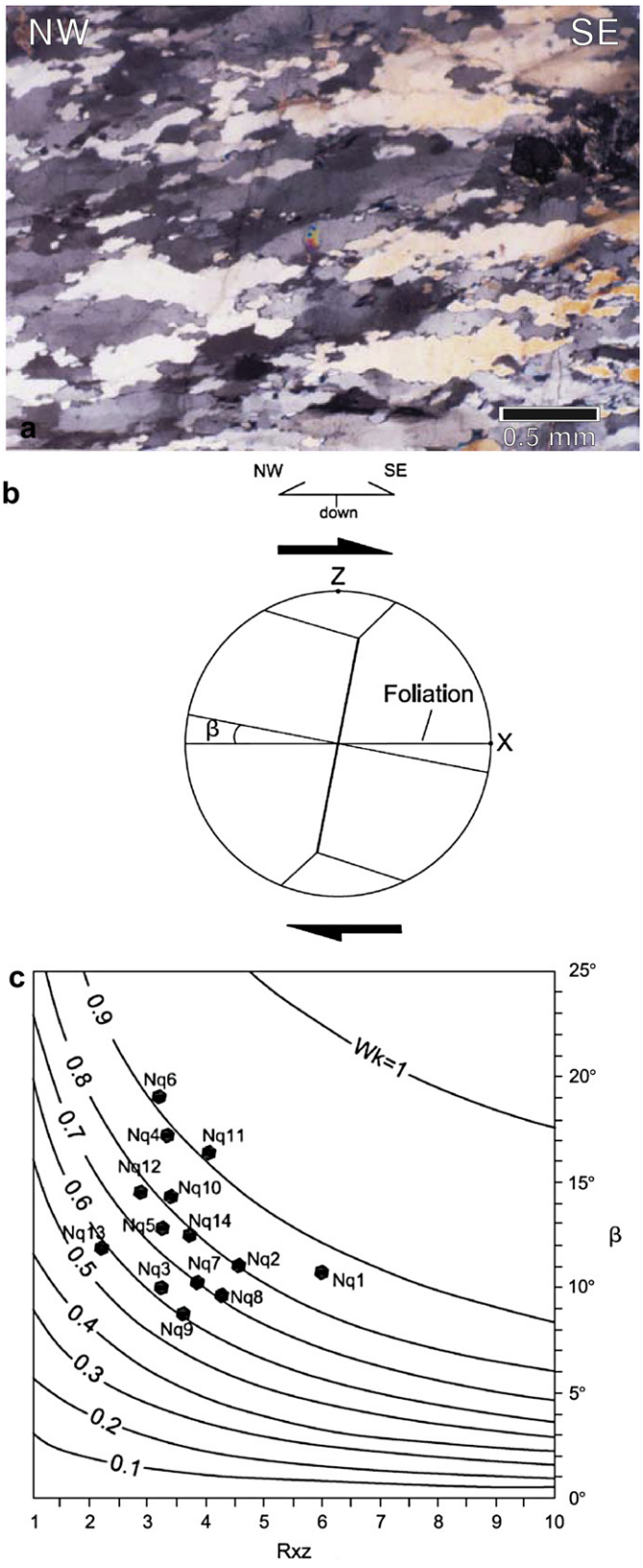

Fig. 8. (a) Photomicrograph of a quartz mylonite from the Sanandaj–Sanandaj metamorphic belt in the study area. Elongate and plastically deformed quartz grains from a well-developed shape-preferred orientation. The quartz grains record evidence of dynamic recrystallization by subgrain rotation and grain boundary migration (location: 29°26′52″ N, 54°36′47″ E). (b) β is the angle between the perpendicular to the central griddle of quartz *c*-axis diagram and the foliation. (c) Plot of β versus R_{xz} (principal normal strain ratio in the *XZ* section) contoured for different W_k. The majority of the measured 14 samples indicate W_k between 0.6 and 0.9.

between the colliding African–Arabian continent and Iranian microcontinent. The arrangement of the Mesozoic ophiolitic complex, tectonic mélange and the distribution of Mesozoic arc-related calc-alkaline granitoid rocks in the Sanandaj–Sirjan metamorphic belt confirm the presence of an ancient subduction zone SW of the Sanandaj–Sirjan metamorphic belt during Mesozoic time (Shahabpour, 2005, 2007). Consumption and closure of the oceanic basin was accomplished during Maastrichtian time and culminated with emplacement of Neyriz ophiolite and pelagic sediments onto the African–Arabian continental margin. The oldest sediments resting unconformably on the Neyriz ophiolite are Late-Cretaceous Tarbur limestone, indicating that the Neyriz ophiolite was obducted by the Late-Cretaceous (Ricou, 1971). Furthermore, $^{40}Ar/^{39}Ar$ heating plateau age from hornblende 92–97 Ma (Haynes and Reynolds, 1980; Babaie et al., 2006) suggest that the tectonic emplacement of Neyriz ophiolite occurred in the Late-Cretaceous. Hornblende grew synkinematically during D1 suggesting that the mylonitic foliation S1, the stretching lineation L1 and the isoclinal folding with fold axes parallel to the L1 formed during exhumation of rock from peak metamorphic conditions. The D2 event is characterized by deformation of the S1 foliation and by the formation of a weaker and less penetrative foliation under lower grade metamorphic conditions. Furthermore, the SW-directed thrusting kinematics facilitating exhumation of rocks during D1 is overprinted by the transpressional dextral strike–slip D2 deformation. The third phase of deformation (D3) developed by localized shear along SW-directed thrusts and post-metamorphic kink bands (documenting ongoing shortening).

6.2. Dextral transpressional event

Given the presence of dextral shear sense indicators such as SC fabrics, mica fish and quartz *c*-axis patterns, we interpret the Zagros Thrust System in the Neyriz area to be overprinted by a dextral transpressional D2 shear zone. The combination of strike–slip and oblique-slip deformation along the Sanandaj–Sanandaj metamorphic belt plus a strong component of pure shear deformation is consistent with a transpressional flow regime (Sanderson and Marchini, 1984; Tikoff and Teyssier, 1994). Dextral transpressional shearing predominantly localized within the metamorphic rocks in the hanging wall of the Main Zagros Thrust. Horizontal to subhorizontal L2 stretching lineations and moderately to steep S2 mylonitic foliations suggest that the metamorphic rocks of the Neyriz area were affected by a dextral strike–slip shear deformation. Many experimental and field investigations have demonstrated that quartz microfabric is a good kinematic and strain path indicator (Simpson and Schmid, 1983; Schmid and Casey, 1986; Mancktelow, 1987). Our analysis of quartz textures from deformed quartz layers within the Sanandaj–Sirjan metamorphic belt suggest plane strain condition during dextral strike–slip shearing under greenschist facies conditions. In addition, our quantitative kinematic vorticity analyses of the quartz texture suggest a major component of pure shear deformation and a stretching component parallel to the deformation zone boundary (i.e. lateral extension). The L2 lineations in the study area are subhorizontal to shallowly plunging towards the SE and all associated semi-quantitative kinematic indicators (oblique boudin trains, SC-, SCC′ fabrics, σ-type geometries) preserve an unequivocal dextral strike–slip sense of shear with a shortening component perpendicular to, and stretching component parallel to the shear zone boundary. This structural pattern shows that the transpressional deformation in the Sanandaj–Sirjan metamorphic belt deviates from the basic model of Sanderson and Marchini (1984), involving both vertical and horizontal stretch components (e.g. Dewey et al., 1998). In confined transpression, as modelled by Sanderson and Marchini (1984) and Fossen and Tikoff (1993), the finite extension

direction for pure-shear dominated transpression is vertical. This is not necessarily the case for unconfined transpression, and the field data from the Sanandaj–Sirjan metamorphic belt in the Neyriz are consistent with a model for unconfined transpression in which lateral extrusion has occurred. Lateral extrusion within transpression zones stabilizes horizontal lineation very effectively in oblique convergence allowing the horizontal lineation to develop even at a high-angle to the convergence direction (Teyssier and Tikoff, 1999). Deformation partitioning in individual zones of different flow geometries allows bulk-flattening strain across the Sanandaj–Sirjan metamorphic belt despite the fact that individual domains appear to be characterized by non-coaxial plane strain deformation. This model is similar to the models which have been proposed by Hudleston (1999) and Teyssier and Tikoff (1999) for maintaining strain compatibility in shear zones. In these models, the maximum extension direction of the pure shear-dominated domains is parallel to the movement direction of the simple shear component.

7. Conclusion

A polyphase deformational history is recorded within the Sanandaj–Sirjan metamorphic belt of the Neyriz area. We infer D1 is related with thrusting an SW directed extrusion of high-grade metamorphic rocks following the oblique collision between the African–Arabian continent and the Iranian microcontinent commencing in the Late-Cretaceous. Deformation patterns imply a transpressional deformation regime within this part of the Zagros orogeny. D2 is superposed on D1 and is dominated by right lateral transpression at greenschist facies conditions. D3 is a post-metamorphic event recording N–S shortening by formation of conjugate kink bands. Mesoscopic and microscopic D2 kinematic indicators revealed unequivocal dextral sense of shear within metamorphic rocks of the Sanandaj–Sirjan metamorphic belt. In more detail, Type-I cross-girdles of quartz *c*-axis fabrics display greenschist facies non-coaxial dextral shear deformation with basal <a> active slip system under plane strain condition in the study area. The quantitatively determined kinematic vorticity number based on the quartz textures is between 0.6 and 0.9 for principal normal strain ratios between 2.5 and 6. Considering the limitations of the method and deformation partitioning in localized shear zones and in different rheologies, it can be concluded that at least some zones of high-strain deformed with a strong pure shear component. Because other semi-quantitative kinematic indicators suggest stretching parallel and shortening perpendicular to the studied right lateral strike–slip zone, we suggest a combined transpression and lateral extrusion model for the study area.

Acknowledgements

We keenly appreciate critical comments and careful reviewing by Professor K. Mulchrone and an anonymous reviewer. We thank Editor Professor J. Hippertt for both his constructive comments and editorial authority. The Research Council of the Shiraz University has supported the project which is gratefully acknowledged. The Structural Processes Group of the Department of Geodynamics and Sedimentology (University of Vienna, Austria) have supported this work, which is gratefully acknowledged. A.F. thanks Austrian Exchange Service (ÖAD) for logistic help during his stay in Vienna. We wish to thank B. Samani, M.R. Heyhat and A.R. Partabian for their help in the fieldwork and laboratory. Important comments by Mike Edwards improved the presentation of the paper.

References

Alavi, M., 1994. Tectonics of the Zagros Orogenic belt of Iran: new data and interpretations. Tectonophysics 229, 211–238.
Alavi, M., 2004. Regional stratigraphy of the Zagros fold-thrust belt of Iran, and its proforeland evolution. American Journal of Science 304, 1–20.
Allen, M.B., Jackson, J., Walker, R., 2004. Late Cenozoic reorganization of the Arabia–Eurasia collision and comparison of the short-term and long-term deformation rates. Tectonics 23, TC2008, doi:10.1029/2003TC001530.
Agard, P., Omrani, J., Jolivet, L., Mouthereau, F., 2005. Convergence history across Zagros (Iran): constraints from collisional and earlier deformation. International Journal of Earth Sciences 94, 401–419.
Avé Lallemant, H.G., Guth, L.R., 1990. Role of extensional tectonics in exhumation of eclogites and blueschists in an oblique subduction setting, northwest Venezuela. Geology 18, 950–953.
Babaie, H.A., Babaei, A., Ghazi, M., Arvin, M., 2006. Geochemical, $^{40}Ar/^{39}Ar$ age and isotopic data for crustal rocks of the Neyriz ophiolite. Iran. Canadian Journal of Earth Sciences 43, 57–70.
Berberian, M., King, G.C., 1981. Towards a palaeogeography and tectonics evolution of Iran. Canadian Journal of Earth Sciences 18, 210–265.
Blanc, E.J.-P., Allen, M.B., Inger, S., Hassani, H., 2003. Structural styles in the Zagros Simple Folded Zone. Iran. Journal of the Geological Society of London 160, 401–412.
Czeck, D.M., Hudleston, P.J., 2003. Testing models for obliquely plunging lineations in transpression: A natural example and theoretical discussion. Journal of Structural Geology 25, 959–982.
Czeck, D.M., Hudleston, P.J., 2004. Physical experiments of vertical transpression with localized nonvertical extrusion. Journal of Structural Geology 26, 573–581.
Díaz Azpiroz, M., Fernández, C., 2005. Kinematic analysis of the southern Iberian shear zone and tectonic evolution of the Acebuches metabasites (SW Variscan Iberian Massif). Tectonics 24, TC3010, doi:10.1029/2004TC001682.
Dewey, J.F., Pitman III, W.C., Ryan, W.B.F., Bonini, J., 1973. Plate tectonics and the evolution of the Alpine System. In: Geological Society of America Bulletin, 84 3137–3180.
Dewey, J.F., Holdsworth, R.E., Strachan, R.A., 1998. Transpression and transtension zones. In: Holdsworth, R.E., Strachan, R.A., Dewey, J.F. (Eds.), Continental Transpressional and Transtensional Tectonics. Special Publication of the Geological Society, London 135, pp. 1–14.
Fossen, H., Tikoff, B., 1993. The deformation matrix for simultaneous simple shearing, pure shearing and volume change, and its application to transpression–transtension tectonics. Journal of Structural Geology 15, 413–422.
Fossen, H., Tikoff, B., 1998. Extended models of transpression and transtension, and application to tectonic settings. In: Holdsworth, R.E., Strachan, R.A., Dewey, J.F. (Eds.), Continental Transpressional and Transtensional Tectonics. Special Publication of the Geological Society, London 135, pp. 15–33.
Goscombe, B.D., Passchier, C.W., 2003. Asymmetric boudins as shear sense indicators: an assessment from field data. Journal of Structural Geology 25, 575–589.
Goscombe, B.D., Passchier, C.W., Hand, M., 2004. Boudinage classification: end-member boudin types and modified boudin structures. Journal of Structural Geology 26, 739–763.
Grasemann, B., Stüwe, K., 2001. The development of flanking folds during simple shear and their use as kinematic indicators. Journal of Structural Geology 23, 715–724.
Grasemann, B., Fritz, H., Vannay, J.C., 1999. Quantitative kinematic flow analysis from the Main Central Thrust Zone (NW-Himalaya, India): implications for a decelerating strain path and the extrusion of orogenic wedges. Journal of Structural Geology 21, 837–853.
Harland, W.B., 1971. Tectonic transpression in Caledonian Spitzbergen. Geological Magazine 108, 27–42.
Haynes, S.J., Reynolds, P.H., 1980. Early development of Tethys and Jurassic ophiolite displacement. Nature 283, 561–563.
Hudleston, P.J., 1999. Strain compatibility in shear zones: is there a problem? Journal of Structural Geology 21 932–932.
Jackson, J.A., McKenzie, D.P., 1984. Active tectonics of Alpine–Himalayan belt between western Turkey and Pakistan. Geophysical Journal of the Royal Astronomical Society 77, 185–264.
Jiang, D., Lin, S., Williams, P.F., 2001. Deformation path in high-strain zones, with reference to slip partitioning in transpressional plate boundary regions. Journal of Structural Geology 23, 991–1005.
Jones, R.R., Holdsworth, R.E., 1998. Oblique simple shear in transpression zones. In: Holdsworth, R.E., Strachan, R.A., Dewey, J.F. (Eds.), Continental Transpressional and Transtensional Tectonics. Geological Society of London, London, pp. 35–40. Special Publication 135.
Jones, R.R., Holdsworth, R.E., Bailey, W., 1997. Lateral extrusion in transpression zones: the importance of boundary conditions. Journal of Structural Geology 19, 1201–1217.
Jones, R.R., Holdsworth, R.E., Clegg, P., McCaffrey, K., Tavarnelli, E., 2004. Inclined transpression. Journal of Structural Geology 26, 1531–1548.
Koop, W.J., Stoneley, R., 1982. Subsidence history of the Middle East Zagros Basin, Permian to Recent. Philosophical Transactions of the Royal Society of London. Series A 305, 149–168.
Law, R.D., 1990. Crystallographic fabrics. A selective review of their applications to research in structural geology. In: Knipe, R.J., Rutter, E.H. (Eds.), Deformation Mechanisms, Rheology and Tectonics. Geological Society, London, pp. 335–352. Special Publications 54.

Lin, S., Jiang, D., Williams, P.F., 1998. Transpression (or transtension) zones of triclinic symmetry: natural example and theoretical modelling. In: Holdsworth, R. E., Strachan, R.A., Dewey, J.F. (Eds.), Continental Transpressional and Transtensional Tectonics. Geological Society of London, London, pp. 41–57. Special Publication 135.

Lisle, R.J., 1985. Geological Strain Analysis. A Manual for the R_f/φ Method. Pergamon Press, New York, 99 pp.

Mancktelow, N.S., 1987. Quartz textures from the Simplon Fault Zone, southwest Switzerland and north Italy. Tectonophysics 135, 133–153.

McClay, K.R., Whitehouse, P.S., Dooley, M., Richards, M., 2004. 3D evolution of fold and thrust belts formed by oblique convergence. Marine and Petroleum Geology 21, 857–877.

McQuarrie, N., 2004. Crustal scale geometry of the Zagros fold-thrust belt, Iran. Journal of Structural Geology 26, 519–535.

Molinaro, M., Leturmy, P., Guezou, J.-C., Frizon de Lamotte, D., 2005. The structure and kinematics of the southeastern Zagros fold-thrust belt; Iran: from thin-skinned to thick-skinned tectonics. Tectonics 24, TC3007, doi:10.1029/2004TC001633.

Müller, M., Grasemann, B., Edwards, M., Voit, K., 2006. Quantitative kinematic flow analysis in an extensional crustal-scale shear zone regime (Kea, Western Cyclades, Greece). PANGEO Austria 2006, Conference Series. Innsbruck University Press. 212-213.

Passchier, C.W., Trouw, R.A.J., 2005. Microtectonics. Springer, Berlin, 366 pp.

Ramberg, H., 1975. Particle paths, displacement and progressive strain applicable to rocks. Tectonophysics 28, 1–37.

Ramsay, J.G., 1967. Folding and Fracturing of Rocks. McGraw-Hill, New York, 568 pp.

Regard, V., Bollier, O., Thomas, J.C., Abbasi, M.R., Mercier, J., Shabanian, E., Feghhi, K., Soleymani, S., 2004. Accommodation of Arabia–Eurasia convergence in the Zagros-Makran transfer zone, SE Iran: a transition between collision and subduction through a young deformation system. In: Tectonics, 23, doi:10.1029/2003TC001599 TC4007.

Ricou, L.E., 1971. Le croissant ophiolitique péri-arabe. Une ceinture de nappes mises en place au Crétacé supérieur. Revue de Géographie Physique et de Géologie Dynamique XIII, 327–350.

Robin, P.Y.F., Cruden, A.R., 1994. Strain and vorticity patterns in ideally ductile transpression zones. Journal of Structural Geology 16, 447–466.

Sanderson, D.J., Marchini, W.R.D., 1984. Transpression. Journal of Structural Geology 6, 449–458.

Sarkarinejad, K., 1999. Tectonic finite strain analysis using Ghuri deformed conglomerate, Neyriz area Southwestern Iran. Iranian Journal of Science and Technology 23, 351–363.

Sarkarinejad, K., Azizi, A., 2008. Slip partitioning and inclined dextral transpression along the Zagros Thrust System, Iran. Journal of Structural Geology 30, 116–136.

Schmid, S.M., Casey, M., 1986. Complete fabric analysis of some commonly observed quartz c-axis patterns. In: Hobbs, B.E., Heard, H.C. (Eds.), Mineral and Rock Deformation. Laboratory Studies-The Paterson Volume. Geophysical Monographs, 36, pp. 263–286.

Sepehr, M., Cosgrove, J.W., 2005. Role of the Kazerun fault zone in the formation and deformation of the Zagros Fold-Thrust Belt, Iran. Tectonics 24, TC5005, doi:10.1029/2004TC001725.

Shahabpour, J., 2005. Tectonic evolution of the orogenic belt in the region located between Kerman and Neyriz. Journal of Asian Earth Sciences 24, 405–417.

Shahabpour, J., 2007. Island-arc affinity of the Central Iranian Volcanic Belt. Journal of Asian Earth Sciences 30, 652–665.

Simpson, C., Schmid, S.M., 1983. An evaluation of criteria to deduce the sense of movement in sheared rocks. Geological Society of America Bulletin 94, 1281–1288.

Stöcklin, J., 1968. Structural history and tectonics of Iran. A review. American Association of Petroleum Geologists Bulletin 52, 1229–1258.

Talebian, M., Jackson, J., 2002. Offset on the Main Recent Fault of NW Iran and implications for late Cenozoic tectonics of the Arabia–Eurasia collision zone. Geophysical Journal International 150, 422–439.

Tatar, M., Hatzfeld, D., Ghafory-Ashtiyani, M., 2004. Tectonics of the Central Zagros (Iran) deduced from microearthquake seismicity. Geophysical Journal International 156, 255–266.

Teyssier, C., Tikoff, B., 1999. Fabric stability in oblique convergence and divergence. Journal of Structural Geology 21, 969–974.

Teyssier, C., Tikoff, B., Markley, M., 1995. Oblique plate motion and continental tectonics. Geology 23, 447–450.

Tikoff, B., Fossen, H., 1995. The limitations of three-dimensional kinematic vorticity analysis. Journal of Structural Geology 12, 1771–1784.

Tikoff, B., Teyssier, C., 1994. Strain modelling of displacement-field partitioning in transpressional orogens. Journal of Structural Geology 16, 1575–1588.

Vernant, P., Nilforoushan, F., Haztfeld, D., Abassi, M., Vigny, C., Masson, F., Nankali, H., Martinod, J., Ashtiany, A., Bayer, R., Tavakoli, F., Chéry, J., 2004. Contemporary crustal deformation and plate kinematics in Middle East constrained by GPS measurement in Iran and northern Oman. Geophysical Journal International 157, 381–398.

Wallis, S.R., 1992. Vorticity analysis in a metachert from the Sanbagawa Belt, SW Japan. Journal of Structural Geology 14, 271–280.

Wallis, S.R., 1995. Vorticity analysis and recognition of ductile extension in the Sanbagawa belt, SW Japan. Journal of Structural Geology 17, 1077–1093.

Ziegler, P.A., Stampfli, G.M., 2001. Late Paleozoic-Early Mesozoic plate boundary reorganization: collapse of the Variscan orogen and opening of Neotethys. In: Cassinis, R. (Ed.), The Continental Permian of the Southern Alps and Sardinia (Italy) Regional Reports and General Correlations, Ed. 25. Annali Museo Civico Science Naturali, Brescia, pp. 17–34.